Available online at www.sciencedirect.com
ScienceDirect
European Journal of Mechanics B/Fluids 27 (2008) 335–345

Gas flow through an elliptical tube over the whole range of the gas rarefaction

Irina Graur [a,*], Felix Sharipov [b]

[a] *Université de Provence, Ecole Polytechnique Universitaire de Marseille, Département de Mécanique Energétique, UMR CNRS 6595, 5 rue Enrico Fermi, 13453 Marseille cedex 13, France*

[b] *Departamento de Física, Universidade Federal do Paraná, Caixa Postal 19044, Curitiba, 81531-990, Brazil*

Received 14 February 2007; received in revised form 20 July 2007; accepted 30 July 2007

Available online 11 August 2007

Abstract

A rarefied gas flow trough a long tube with an elliptical cross section is studied on the basis of the BGK kinetic model equation in the whole range of the Knudsen number varying from the free molecular regime to the hydrodynamic one. A wide range of the aspect ratio is considered. The mass flow rate is calculated as a function of the pressures on the tube ends.

Keywords: Rarefied gas; Knudsen number; Microchannels; Boltzmann equation

1. Introduction

Rarefied gas flows through capillaries of different forms are very important in practice. Many industrial apparatuses such as microducts, microturbines or vacuum equipment are the examples of small devices involving the gas flow at an arbitrary Knudsen number. Recently, various numerical methods were developed and applied to rarefied gas flows through capillaries. Such flows through capillary of simple forms, e.g. circular tube, plane channel, were profoundly studied by many researchers. A critical review and recommended data on this topic can be found in Ref. [1]. Recently, some results on gas flows through a rectangular channel *obtained by the discrete velocity method* were reported in Refs. [3,4]. Numerical schemes applied in these papers are suitable just only for the specific capillary cross section, i.e. for circle or for rectangle. However, the wide diversity of the capillary forms used in practice requires a further development of the existing approaches so that it would be possible to calculate gas flows through capillaries of arbitrary form, e.g. ellipse, triangle, trapezoid etc. Some results obtained by the integro-moment method based on the linearized BGK equation for tubes with various cross sections are reviewed in Ref. [5]. According to this review, a rarefied gas flow through a tube with an elliptical cross section was *calculated* in Ref. [6] only for one value of the aspect ratio by the integro-moment method. Earlier this method was applied also to the gas flow through a rectangular long channel in Ref. [2].

* Corresponding author.
E-mail addresses: Irina.Graour@polytech.univ-mrs.fr (I. Graur), sharipov@fisica.ufpr.br (F. Sharipov).
URL: http://fisica.ufpr.br/sharipov (F. Sharipov).

0997-7546/$ – see front matter
doi:10.1016/j.euromechflu.2007.07.003

The aim of the present paper is to calculate the gas flow through a tube with an elliptical cross section over the whole range of the Knudsen number and in a wide range of the aspect ratio. Moreover, we apply the discrete velocity method [7] successfully used for such kind problems in many previous works, see e.g. Refs. [8–10]. The elliptical cross section does not have the axial symmetry in contrast to that of circular tube and it does not allow to apply a uniform grid used for rectangular channel. Thus, a consideration of the elliptical cross section is the first step to a general approach based on the discrete velocity method suitable for any form of the capillary cross section in all regimes of the gas flow including the hydrodynamic, transitional and free molecular ones. A special attention is paid to the slip regime, for which a simple formula of the mass flow rate is obtained.

2. Statement of the problem

Consider a tube connecting two reservoirs containing the same gas and maintained at the same temperature T. The tube cross section is elliptical as is shown in Fig. 1, where $2b$ is the maximal tube dimension in the y direction, $2a$ is the maximal dimension in the x direction. Without the lost of generality, we consider that $b \leqslant a$. The pressure in the left and in the right reservoirs are equal p_1 and p_2, respectively. We are going to calculate the mass flow rate through this tube assuming that:

- The tube length L is significantly larger than the dimension a of the tube cross section, i.e. $a \ll L$. This assumption allows us to neglect the end effects and to consider only the longitudinal component of the bulk velocity, which depends only on x and y coordinates.
- The pressure depends only on the longitudinal coordinate z' and its gradient is small, i.e.

$$\xi = \frac{b}{p}\frac{\mathrm{d}p}{\mathrm{d}z'}, \qquad |\xi| \ll 1. \tag{1}$$

This assumption allows us to linearize the kinetic equation.

The gas rarefaction is characterized by the parameter

$$\delta = \frac{bp}{\mu v_m}, \quad v_m = \left(\frac{2kT}{m}\right)^{1/2}, \tag{2}$$

where μ is the stress viscosity, v_m is the most probable molecular speed, m is the molecular mass of the gas, and k is the Boltzmann constant. Since the viscosity is proportional to the molecular mean free path, the rarefaction parameter δ is inversely proportional to the Knudsen number. The results of the mass flow rate $\dot{M}$ will be presented in terms of the reduced flow rate G_P defined as

$$G_P = -\frac{v_m}{\pi abp\xi}\dot{M}. \tag{3}$$

Let us introduce the following dimensionless quantities

$$x = \frac{x'}{b}, \qquad y = \frac{y'}{b}, \qquad z = \frac{z'}{b}, \qquad u = \frac{u'_z}{v_m\xi}, \tag{4}$$

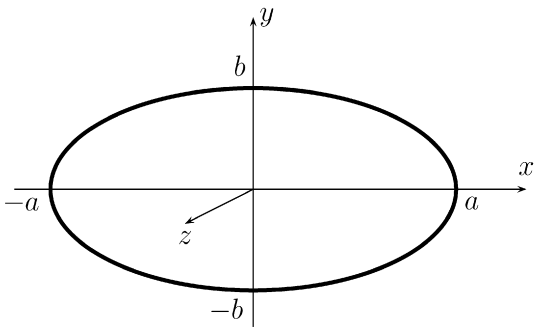

Fig. 1. Tube cross section and coordinates.

where u'_z is the z component of the bulk velocity. Then the reduced flow rate G_P defined by Eq. (3) can be calculated via the dimensionless velocity $u(x, y)$ as

$$G_P = -\frac{2}{\pi}\frac{b}{a}\int_{-1}^{1}\int_{-a/b\sqrt{1-y^2}}^{a/b\sqrt{1-y^2}} u(x, y)\,\mathrm{d}x\,\mathrm{d}y. \tag{5}$$

In order to compare the present results with those corresponding to the gas flow between two parallel plates it is interesting to introduce the flow rate along a symmetry axis, i.e. at $x = 0$, as follows

$$G_{P0} = -\int_{-1}^{1} u(0, y)\,\mathrm{d}y. \tag{6}$$

It is expected that in the limit of high aspect ratio, i.e. at $a/b \to \infty$, this flow rate tends to that corresponding to the parallel plates [1].

3. Hydrodynamic regime of flow

In the hydrodynamic regime ($\delta \to \infty$) the gas flow is described by the Stokes equation which reads

$$\frac{\partial^2 u'_z}{\partial x'^2} + \frac{\partial^2 u'_z}{\partial y'^2} = \frac{1}{\mu}\frac{\mathrm{d}p}{\mathrm{d}z'}. \tag{7}$$

With the help of Eqs. (2)–(4) its dimensionless form is obtained

$$\frac{\partial^2 u}{\partial x^2} + \frac{\partial^2 u}{\partial y^2} = \delta. \tag{8}$$

If we assume the non-slip boundary condition

$$u(x, y)\big|_E = 0, \tag{9}$$

where the curve E is determined by the ellipse equation $x^2\frac{b^2}{a^2} + y^2 = 1$, then Eq. (8) is solved analytically [11]

$$u(x, y) = \frac{\delta}{2}\frac{a^2}{a^2 + b^2}\left(x^2\frac{b^2}{a^2} + y^2 - 1\right). \tag{10}$$

Substituting this expression into Eq. (5) the reduced mass flow rate is calculated as

$$G_P^H = \frac{\delta}{2}\frac{a^2}{a^2 + b^2}, \tag{11}$$

where the superscript H is attached to emphasize that this is the hydrodynamic solution. The flow rate G_P^H calculated for the different sections aspect ratio a/b is given in Table 1. In the limit of cylindrical tube $a/b = 1$ the expression (11) coincides with that obtained for this case in Ref. [1], i.e. $G_P = \delta/4$. However, in the limit of wide tube $a/b \to \infty$ the flow rate G_P^H does not tend to that value obtained for a gas flow between two parallel plates.

Substituting Eq. (10) into (6) the flow rate at $x = 0$ is obtained as

$$G_{P0}^H = \frac{2\delta}{3}\frac{a^2}{a^2 + b^2}. \tag{12}$$

Table 1
Reduced flow rate G_P^H and slip correction S vs aspect ratio b/a

a/b	1	1.01	1.1	2	5	10	20	50	100	∞
G_P^H/δ	0.25	0.2525	0.2738	0.4	0.4808	0.4950	0.4987	0.4998	0.4999	0.5
S	1.	1.0050	1.0482	1.3518	1.6198	1.6770	1.6924	1.6968	1.6974	1.6976

It can be seen that this flow rate tends to the limit value corresponding to the plane flow between two plates [1], i.e.

$$\lim_{a/b\to\infty} G^H_{P0} = \frac{2\delta}{3}. \tag{13}$$

Note, here all lengths are measured in the units of b, while the distance between the plates is usually used in the problem of the plane gas flow. Thus, the factor 4 appears in Eq. (13) compared with the results presented in Ref. [1].

4. Velocity slip correction

A moderate rarefaction of the gas can be taken into account applying the velocity slip boundary condition [12] to the Stokes equation. In other words, we consider that the tangential component of the bulk velocity near the wall is proportional to its normal gradient, i.e.

$$u = \sigma_{\rm P}\ell\frac{\partial u}{\partial \eta'}, \quad \text{at } \eta' = 0, \tag{14}$$

where η' is the normal coordinate with its origin at the tube wall and directed toward to the gas, $\sigma_{\rm P}$ is the viscous slip coefficient, $\ell = \mu\, v_m/p$ is the equivalent mean free path. The bulk velocity u may be decomposed as

$$u(x, y) = u_H(x, y) + \sigma_{\rm P} u_s(x, y), \tag{15}$$

where $u_H(x, y)$ is the hydrodynamic solution (10) and $u_s(x, y)$ is the slip correction. Since both velocities $u(x, y)$ and $u_H(x, y)$ satisfy the Stokes equation (8), the slip velocity correction $u_s(x, y)$ must satisfy the corresponding homogeneous equation

$$\frac{\partial^2 u_s}{\partial x^2} + \frac{\partial^2 u_s}{\partial y^2} = 0. \tag{16}$$

Substituting Eq. (15) into (8), taking into account the boundary condition (9) for the hydrodynamic velocity u_H one obtains the boundary condition for u_s as

$$u_s(x, y) = \frac{1}{\delta}\frac{\partial u_H(x, y)}{\partial \eta}\bigg|_E, \tag{17}$$

where $\eta = \eta'/a$ is the dimensionless normal coordinate. Since the velocity u_H is proportional to δ (see Eq. (10)), both sides of Eq. (17) are of the zero order with respect to δ, while the terms of the order $1/\delta$ are neglected. Calculating the normal derivative $\partial u_H/\partial\eta$ from Eq. (10), the slip condition (17) is obtained as

$$u_s(x, y)|_E = -\left[x^2\left(1 - \frac{a^2}{b^2}\right) + \frac{a^4}{b^4}\right]^{1/2}\left[1 + \frac{a^2}{b^2}\right]^{-1}. \tag{18}$$

Substituting Eq. (15) into the expression (5) the mass flow rate may be represented in the form

$$G_P = G^H_P + \sigma_p S, \tag{19}$$

where G^H_P is given by Eq. (11) and the flow rate due to the slip correction S is calculated via the velocity u_s as

$$S = -\frac{2}{\pi}\frac{b}{a}\int_{-1}^{1}\int_{-a/b\sqrt{1-y^2}}^{a/b\sqrt{1-y^2}} u_s(x, y)\,{\rm d}x\,{\rm d}y. \tag{20}$$

Eq. (16) with the boundary condition (17) is solved numerically. The second order finite-difference scheme is used for the approximation of the space derivatives in (16). The corresponding system of the linear equations is solved applying the Gauss elimination method. The values of the slip correction S calculated for various aspect ratios are presented in Table 1.

The numerical results for the slip flow rate S given in Table 1 are well interpolated by the formula

$$S = 1 - 0.6976\frac{1 - (a/b)^2}{1.951 + (a/b)^2} \tag{21}$$

obtained by the least-square technique. Substituting Eqs. (11) and (21) into (19) we obtain

$$G_P = \frac{\delta}{2}\frac{a^2}{a^2+b^2} + \sigma_P\left[1 - 0.6976\frac{1-(a/b)^2}{1.951+(a/b)^2}\right]. \tag{22}$$

It should be noted that the solution of Eq. (16) with (17) depends neither on the parameter δ nor on the slip coefficient σ_P. Thus, the expression (22) can be used with any slip coefficients including those obtained for the non-diffuse gas–surface interaction [12] and for gaseous mixtures [13].

5. Kinetic equation

To calculate the flow rate G_P in the transition regime the Boltzmann equation should be solved. This equation provides reliable numerical data but requires great computational efforts. To reduce these efforts the collision integral may be simplified remaining its main properties applying one of the model kinetic equations like BGK, S-model or ellipsoidal model. Since we are interested only in the isothermal flow in the present paper we applied the BGK kinetic model equation, which for a steady flow reads [14]

$$\mathbf{v}\cdot\frac{\partial f}{\partial \mathbf{r}'} = \frac{f^M - f}{\tau}, \tag{23}$$

where f is the velocity distribution function, $\mathbf{r}'$ is the position vector, $\mathbf{v}$ is the molecular velocity, f^M is the local Maxwellian distribution function:

$$f^M(n,T,\mathbf{u}') = n(\mathbf{r}')\left[\frac{m}{2\pi kT(\mathbf{r}')}\right]^{3/2}\exp\left[-\frac{m(\mathbf{v}-\mathbf{u}'(\mathbf{r}'))^2}{2kT(\mathbf{r}')}\right], \tag{24}$$

here n is the number density, $\mathbf{u}'$ is the bulk velocity defined as

$$\mathbf{u}'(\mathbf{r}') = \frac{1}{n}\int \mathbf{v} f(\mathbf{r}',\mathbf{v})\,\mathrm{d}\mathbf{v}. \tag{25}$$

The relaxation time expression

$$\tau = \frac{\mu}{p} \tag{26}$$

provides the best agreement with the exact Boltzmann equation for isothermal rarefied gas flows.

Under the assumptions of the small local pressure gradients (1) the distribution function f can be linearized as

$$f(\mathbf{r},\mathbf{c}) = f^0(c)\big[1+\xi\big(z+h(x,y,\mathbf{c})\big)\big], \tag{27}$$

where $\mathbf{c} = \mathbf{v}/v_m$ is the dimensionless molecular velocity, h is the perturbation function, f^0 is the absolute Maxwellian

$$f^0(c) = n_0\left(\frac{m}{2\pi kT}\right)^{3/2}\mathrm{e}^{-c^2} \tag{28}$$

with the equilibrium number density n_0. Substituting Eq. (27) into Eq. (23) and using Eqs. (2) and (26) we obtain the linearized BGK equation

$$c_x\frac{\partial h}{\partial x} + c_y\frac{\partial h}{\partial y} = \delta\big[2c_z u - h(x,y,\mathbf{c})\big] - c_z, \tag{29}$$

where

$$u = \frac{1}{\pi^{3/2}}\int c_z\,\mathrm{e}^{-c^2}h(x,y,\mathbf{c})\,\mathrm{d}\mathbf{c} \tag{30}$$

obtained from Eqs. (4) and (25). Multiplying Eq. (29) by $\frac{c_z}{\sqrt{\pi}}\mathrm{e}^{-c_z^2}$ and integrating it with respect to c_z we obtain

$$c_x\frac{\partial \phi}{\partial x} + c_y\frac{\partial \phi}{\partial y} = \delta\big[u - \phi(x,y,c_x,c_y)\big] - \frac{1}{2}, \tag{31}$$

where the function ϕ is introduced in order to eliminate the variable c_z

$$\phi(x, y, c_x, c_y) = \frac{1}{\sqrt{\pi}} \int_{-\infty}^{+\infty} c_z \mathrm{e}^{-c_z^2} h \, \mathrm{d}c_z. \tag{32}$$

The bulk velocity is expressed via ϕ as

$$u(x, y) = \frac{1}{\pi} \int_{-\infty}^{+\infty} \int_{-\infty}^{+\infty} \mathrm{e}^{-c_x^2 - c_y^2} \phi(x, y, c_x, c_y) \, \mathrm{d}c_x \, \mathrm{d}c_y. \tag{33}$$

To simplify the solution of Eq. (31) the Cartesian coordinates in the velocity space (c_x, c_y) are replaced by the polar coordinates (c_p, φ), i.e.

$$c_x = c_p \cos\varphi, \qquad c_y = c_p \sin\varphi, \tag{34}$$

where $0 \leqslant c_p < \infty$ and $0 \leqslant \varphi \leqslant 2\pi$. Then Eq. (31) is written down in the new variables as

$$-c_p \frac{\partial \phi}{\partial s} = \delta\big[u - \phi(x, y, c_p, \varphi)\big] - \frac{1}{2}, \tag{35}$$

where s is the characteristics, i.e. the distance from the point (x, y) in the direction opposite to the two dimensional velocity vector (c_x, c_y). The bulk velocity is expressed as

$$u(x, y) = \frac{1}{\pi} \int_0^{2\pi} \int_0^{\infty} \phi(x, y, c_p, \varphi) \mathrm{e}^{-c_p^2} c_p \, \mathrm{d}c_p \, \mathrm{d}\varphi. \tag{36}$$

We assume the complete accommodation of the molecules on the tube walls. This means that $h = 0$ at the walls for the reflected particles. Consequently, the condition $\phi = 0$ for the reflected particles is used as the boundary condition for Eq. (35).

6. Free molecular regime

In the free molecular regime ($\delta = 0$) Eq. (35) is significantly simplified and can be solved analytically. After its integration along the characteristics the perturbation function ϕ takes the form

$$\phi(x, y, c_p, \varphi) = -\frac{s_E(x, y, \varphi)}{2c_p}, \tag{37}$$

where s_E is the distance from the point (x, y) to the ellipse boundary in the direction opposite to the molecular velocity, i.e.

$$s_E = \left[\frac{(y - x\tan\varphi)\tan\varphi + \operatorname{sign}(\cos\varphi)\sqrt{(\tan\varphi)^2 - \frac{(y - x\tan\varphi)^2 - 1}{(a/b)^2}}}{(b/a)^2 + (\tan\varphi)^2} + x \right] \frac{1}{\cos\varphi}. \tag{38}$$

Substituting Eq. (37) with (38) into (36) the bulk velocity is obtained

$$u(x, y) = -\frac{1}{4\sqrt{\pi}} \int_0^{2\pi} s_E(x, y, \varphi) \, \mathrm{d}\varphi. \tag{39}$$

Then the flow rate is calculated by Eq. (5). Such an integration was carried out numerically and the corresponding results are shown in the first row of Table 2.

Table 2
Reduced flow rate G_P vs rarefaction parameter δ and aspect ratio a/b

δ	G_P, Refs. [16,17]	G_P, present work								
	$a/b = 1$	$a/b = 1$	1.01	1.1	2	5	10	20	50	100
0	–	1.505	1.512	1.577	2.066	2.889	3.540	4.199	5.075	5.739
0.01	1.4760	1.477	1.485	1.548	2.015	2.769	3.314	3.794	4.275	4.504
0.02	1.4598	1.460	1.468	1.529	1.985	2.705	3.198	3.598	3.946	4.080
0.05	1.4295	1.430	1.437	1.497	1.935	2.591	2.994	3.272	3.459	3.511
0.1	1.4026	1.403	1.410	1.469	1.893	2.492	2.817	3.006	3.107	3.130
0.2	1.3816	1.381	1.388	1.446	1.861	2.403	2.651	2.770	2.821	2.831
0.5	1.3864	1.386	1.393	1.455	1.881	2.365	2.534	2.596	2.618	2.622
0.8	1.4252	1.425	1.432	1.499	1.951	2.424	2.565	2.612	2.628	2.631
1.0	1.4583	1.458	1.466	1.536	2.009	2.482	2.614	2.657	2.670	2.673
1.5	1.5532	1.553	1.562	1.641	2.170	2.658	2.780	2.817	2.829	2.830
2.0	1.6576	1.657	1.667	1.757	2.344	2.857	2.976	3.012	3.023	3.024
5.0	2.3483	2.348	2.365	2.516	3.471	4.188	4.331	4.371	4.383	4.385
10.0	3.5633	3.563	3.593	3.850	5.430	6.532	6.738	6.796	6.812	6.815
20.0	6.0411	6.041	6.095	6.565	9.402	11.30	11.65	11.74	11.77	11.77
30.0	8.5333	8.532	8.612	9.294	13.39	16.09	16.58	16.71	16.75	16.75
40.0	11.0295	11.03	11.13	12.03	17.39	20.89	21.52	21.69	21.74	21.74
50.0	13.5269	13.52	13.65	14.76	21.38	25.69	26.46	26.66	26.72	26.72

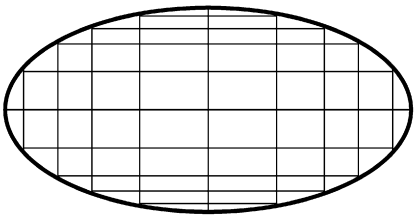

Fig. 2. Non-uniform grid in physical space.

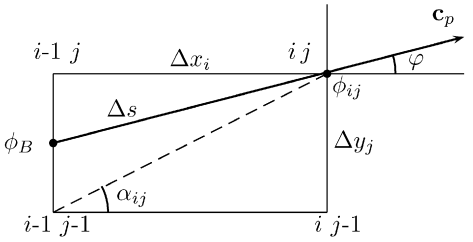

Fig. 3. Scheme of finite difference, see Eq. (41).

7. Transitional regime

According to the discrete velocity method a grid in the velocity space (c_p, φ) is introduced. For the variable c_p the Gaussian abscissas corresponding to the weight function

$$W(c_p) = \frac{1}{\pi} e^{-c_p^2} c_p \tag{40}$$

are used, while a uniform grid is introduced for the variable φ. In the physical space a non-uniform grid is introduced in x and y directions in order to obtain the grid lines intersections on the ellipse boundary as is shown in Fig. 2. Let us note α_{ij} the angle characterizing the grid cells, so that $\tan\alpha_{ij} = \Delta y_j / \Delta x_i$ as is shown in Fig. 3. The explicit finite difference scheme for the function ϕ at the fixed point (c_p, φ) of the velocity space has the following form (see Fig. 3):

$$\phi_{ij}(c_p, \varphi) = \frac{\delta u_{ij} - \frac{1}{2} + \frac{c_p}{\Delta s}\phi_B(c_p, \varphi)}{\delta + \frac{c_p}{\Delta s}}, \tag{41}$$

where $\phi_{ij}(c_p, \varphi) = \phi(x_i, y_j, c_p, \varphi)$,

$$\Delta s = \begin{cases} \Delta x_i / \cos\varphi & \text{at } \varphi \leqslant \alpha_{ij}, \\ \Delta y_j / \sin\varphi & \text{at } \varphi > \alpha_{ij}. \end{cases} \tag{42}$$

The value of the function $\phi_B(c_p, \varphi)$ is calculated as the linear interpolation of ϕ in the two nearest points of the grid

$$\phi_B(c_p, \varphi) = \begin{cases} (1 - T_{ij})\phi_{i-1\,j} + T_{i,j}\phi_{i-1\,j-1}, & \text{at } \varphi \leqslant \alpha_{ij}, \\ (1 - 1/T_{ij})\phi_{ij-1} + (1/T_{ij})\phi_{i-1\,j-1} & \text{at } \varphi > \alpha_{ij}, \end{cases} \tag{43}$$

where $T_{ij} = \tan\varphi/\tan\alpha_{ij}$. Because of the flow symmetry the calculations can be carried out only in the range $0 \leqslant \varphi \leqslant \pi/2$, but over the whole physical space.

For the first iteration the function u is assumed to be known. When Eq. (41) is solved for all combinations c_{pk} and φ_m, then the new quantities of u are calculated according to Eq. (36). The quadrature for the velocity has the following form

$$u_{ij} = \sum_{k=1}^{N_c} \sum_{m=1}^{N_\varphi} \phi_{ij}(c_{pk}, \varphi_m) W_k \Delta\varphi, \tag{44}$$

c_{pk} and W_k are the Gaussian abscissas and weights, respectively. N_c and N_φ are number of points for the variables c_p and φ, respectively.

To reduce the computational efforts near the hydrodynamic regime, i.e. at $\delta \geqslant 10$, the optimization proposed in Ref. [7] was used. The perturbation function is decomposed into two parts

$$h(x, y, \mathbf{c}) = h_H(x, y, \mathbf{c}) + \tilde{h}(x, y, \mathbf{c}), \tag{45}$$

where

$$h_H(x, y, \mathbf{c}) = \lim_{\delta\to\infty} h(x, y, \mathbf{c}), \tag{46}$$

and $\tilde{h}(x, y, \mathbf{c})$ vanishes when δ tends to infinity. The function $h_H(x, y, \mathbf{c})$ corresponding to the continuum solution can be found by the Chapman–Enskog method [15] retaining only the dominant term

$$h_H(x, y, \mathbf{c}) = 2c_z u_H, \tag{47}$$

where the velocity u_H is defined by relation (10). Substituting (45) into (29) we obtain the equation for $\tilde{h}$:

$$c_x \frac{\partial\tilde{h}}{\partial x} + c_y \frac{\partial\tilde{h}}{\partial y} = \delta(2c_z\tilde{u} - \tilde{h}) - c_z - 2\delta c_z \frac{xc_x + (a/b)^2 y c_y}{1 + (a/b)^2}, \tag{48}$$

where

$$\tilde{u} = \frac{1}{\pi^{3/2}} \int \mathrm{e}^{-c^2} c_z \tilde{h}(x, y, \mathbf{c})\, \mathrm{d}\mathbf{c}. \tag{49}$$

Then Eq. (48) is solved by exactly the same method as Eq. (29).

8. Numerical results

The numerical calculations were carried out in the range of the rarefaction parameter δ from 0.01 to 50 and for several values of the aspect ration a/b in the range from 1 to 100. The flow rate G_P was calculated with the numerical error less than 0.1%. The accuracy was estimated by comparing numerical results obtained for different parameters of the numerical grid. An analysis showed that to reach the accuracy of 0.1% the grid in the physical space should be 1000×1000 points and the parameter N_φ should be equal to 100 for all values of δ, while the parameter N_c depends on δ. In the range $0 \leqslant \delta \leqslant 0.1$ the value $N_c = 25$ should be used and for $\delta > 0.1$ the smaller value, viz. $N_c = 12$, is enough. The numerical results on the flow rate G_P are presented in Table 2. In the case $a/b = 1$, i.e. circular cross section of the tube, the results of the present work are compared with those obtained from the BGK equation by the integro-moment method in Ref. [16] and by so called F_N method in Ref. [17]. It can be seen that the discrepancy between the results obtained by two different method does not exceed the numerical accuracy.

In the fourth and fifth columns of Table 2 the results corresponding to a small deviation from the circular tube are shown, i.e. for a/b =1.01 and 1.1, respectively. Note, in the hydrodynamic regime ($\delta \gg 1$) the relative difference of the flow rate due to the deviation of the aspect ratio from unity is about $(a/b - 1)$, while near the free molecular regime $\delta \ll 1$ this relative difference is quite smaller than $(a/b - 1)$.

For the large values of the aspect ratio, i.e. at $a/b \gg 1$ the flow rate G_P tends to a constant values in the hydrodynamic regime ($\delta \gg 1$). The same conclusion can be made from the slip solution (22), and from Table 1 where it is shown that both G_P/δ and S tend to a constant when a/b tends to infinity. Near the free molecular regime $\delta \ll 1$ the flow rate increases by increasing the aspect ratio. In all regimes the flow rate G_p does not tend to that corresponding to gas flow between two parallel plates.

Table 3
Reduced flow rate G_{P0} vs rarefaction parameter δ and aspect ratio a/b

δ	G_{P0}, present work					Ref. [16]
	$a/b = 5$	10	20	50	100	∞
0	12.77	15.82	18.92	23.04	26.14	∞
0.01	3.074	3.729	4.314	4.908	5.192	12.20
0.1	2.819	3.232	3.472	3.588	3.609	8.131
1.0	2.954	3.117	3.171	3.179	3.188	6.155
10.0	8.414	8.690	8.769	8.782	8.793	11.07
50.0	33.93	34.96	35.22	35.30	35.37	37.48

The numerical results on the flow rate G_{P0} in the axis of the tube, i.e. at $x = 0$, for some values of the rarefaction parameter δ and for large values of the aspect ratio a/b are presented in Table 3. In the last column of the same table the results corresponding to the gas flow between two parallel plates reported in Ref. [16] are shown. Note, the results of Ref. [16] were multiplied by the factor 4. It is surprise that the flow rate G_{P0} does not tend to the value corresponding to the parallel plates at any finite value of the rarefaction parameter δ. According to Eqs. (12) and (13) the quantity G_{P0} tends to that for the parallel plates only in the hydrodynamic regime ($\delta \to \infty$). It can be explained by the fact that the local equilibrium is fulfilled in the hydrodynamic regime and the flow rate G_{P0} depends only on the conditions near the line $x = 0$, where the wall of the elliptical tube are almost flat for a large aspect ratio a/b. In the transition ($\delta \sim 1$) and free molecular ($\delta = 0$) regimes the local equilibrium is broken and the flow rate G_{P0} becomes dependent on the conditions over the whole cross section. That is why even for large value of a/b the influence of the small curvature upon the quantity G_{P0} is significant in the transition and free molecular regimes.

9. Arbitrary pressure drop

In Section 2 it was noted that the reduced flow rate G_P defined by Eq. (3) depends on the longitudinal coordinate through the local pressure values. From a practical point of view, it is difficult to utilize the calculated mass flow rates using the dimensionless form (3) because the local pressure and local rarefaction parameter are unknown along the channel. To calculate the flow rate as function of the pressure drop on the tube ends we introduce the quantity

$$G_{\Delta P} = \frac{L v_m}{b^2 a (p_1 - p_2)} \dot{M}, \tag{50}$$

which is determined by the rarefaction parameters on the tube ends, i.e. by

$$\delta_1 = \frac{b p_1}{\mu v_m}, \quad \text{and} \quad \delta_2 = \frac{b p_2}{\mu v_m}. \tag{51}$$

Substituting Eq. (3) into (50) the relation between $G_{\Delta P}$ and G_P is obtained [3,18]

$$G_{\Delta P}(\delta_1, \delta_2) = \frac{1}{\delta_2 - \delta_1} \int_{\delta_1}^{\delta_2} G_P(\delta)\, \mathrm{d}\delta. \tag{52}$$

Some values of the flow rate $G_{\Delta P}$ calculated numerically by the integration (52) are given in Table 4. By analyzing the data shown in Tables 2 and 4 we conclude that the formula

$$G_{\Delta P}(\delta_1, \delta_2) = G_P\left(\frac{\delta_1 + \delta_2}{2}\right) \tag{53}$$

works very well when b/a is close to unity for the whole range of the rarefaction parameter δ. The same conclusion was made in Ref. [18] for the tube of the cylindrical cross section and in Ref. [3] for the square cross section channel. However, for the large values of the aspect ratio a/b the expression (53) does not provide a reasonable approximation, especially for the small and transitional values of δ_2. This happens because of the deep Knudsen minimum. Thus, for large values of a/b the calculation of the flow rate $G_{\Delta P}$ must be performed only by the numerical integration according to Eq. (52).

Table 4
Reduced flow rate $G_{\Delta P}$ vs rarefaction parameters δ_1, δ_2 and aspect ratio a/b

δ_1	δ_2	$G_{\Delta P}$		
		$a/b = 1$	10	100
0	0.1	1.438	3.049	3.741
0	1.0	1.406	2.637	2.807
0	10.	2.373	4.404	4.474
0	40.	6.057	11.68	11.81
0.1	1.0	1.403	2.591	2.703
0.1	10.	2.382	4.418	4.481
0.1	40.	6.068	11.70	11.83
1.0	10.	2.480	4.600	4.659
1.0	40.	6.176	11.91	12.04

10. Conclusion

The mass flow rate trough a tube with the elliptical cross section is calculated over the whole range of the rarefaction parameter varying from the free molecular regime to the hydrodynamic one. Various aspect ratios of the tube axis a/b are considered. The analysis of the numerical data shows the significant influence of this aspect ratio on the mass flow rate. The Knudsen minimum in the transitional regime exists at any aspect ratio a/b. It is becomes deeper by the decreasing ratio a/b. It is shown that for large values of a/b the flow rate does not tend to that corresponding to the gas flow between to parallel plates. The simple formula (22) for calculation of the mass flow rate in the slip regime is proposed. To calculate the flow rate at any pressure ratio p_1/p_2 the approximate formula (53) can be used only for the ratio a/b close to unity.

Acknowledgement

This work was realized in the frame of Cooperation Agreement between Conselho Nacional de Desenvolvimento Científico e Tecnológico (CNPq, Brazil) and Centre National de la Recherche Scientifique (CNRS, France). The authors acknowledge the support of their research by these foundations.

References

[1] F. Sharipov, V. Seleznev, Data on internal rarefied gas flows, J. Phys. Chem. Ref. Data 27 (3) (1998) 657–706.
[2] S.K. Loyalka, T.S. Storvick, H.S. Park, Poiseuille flow and thermal creep flow in long, rectangular channel in the molecular and transition flow regimes, J. Vac. Sci. Technol. 13 (6) (1976) 1188–1192.
[3] F. Sharipov, Rarefied gas flow through a long rectangular channel, J. Vac. Sci. Technol. A 17 (5) (1999) 3062–3066.
[4] F. Sharipov, Non-isothermal gas flow through rectangular microchannels, J. Micromech. Microeng. 9 (4) (1999) 394–401.
[5] K. Aoki, Numerical analysis of rarefied gas flows by finite-difference method, in: E.P. Muntz, D.P. Weaver, D.H. Campbell (Eds.), 16th Int. Symp., in: Rarefied Gas Dynamics, vol. 118, Washington, 1989, American Institute of Aeronautics and Astronautics, 1989, pp. 297–322.
[6] M. Hasegawa, Y. Sone, Poiseuille and thermal transpiration flows of rarefied gas for various pipes, J. Vac. Soc. Japan 31 (1988) 416–419 (in Japanese).
[7] F.M. Sharipov, E.A. Subbotin, On optimization of the discrete velocity method used in rarefied gas dynamics, Z. Angew. Math. Phys. (ZAMP) 44 (1993) 572–577.
[8] F. Sharipov, Application of the Cercignani–Lampis scattering kernel to calculations of rarefied gas flows. III. Poiseuille flow and thermal creep through a long tube, Eur. J. Mech. B/Fluids 22 (2003) 145–154.
[9] S. Naris, D. Valougeorgis, F. Sharipov, D. Kalempa, Discrete velocity modelling of gaseous mixture flows in MEMS, Superlattices and Microstructures 35 (2004) 629–643.
[10] S. Naris, D. Valougeorgis, D. Kalempa, F. Sharipov, Flow of gaseous mixtures through rectangular microchannels driven by pressure, temperature and concentration gradients, Phys. Fluids 17 (10) (2005) 100607.1–100607.12.
[11] L.D. Landau, E.M. Lifshitz, Fluid Mechanics, Pergamon, New York, 1989.
[12] F. Sharipov, Application of the Cercignani-Lampis scattering kernel to calculations of rarefied gas flows. II. Slip and jump coefficients, Eur. J. Mech. B/Fluids 22 (2003) 133–143.
[13] F. Sharipov, D. Kalempa, Velocity slip and temperature jump coefficients for gaseous mixtures. I. Viscous slip coefficient, Phys. Fluids 15 (6) (2003) 1800–1806.
[14] P.L. Bhatnagar, E.P. Gross, M.A. Krook, A model for collision processes in gases, Phys. Rev. 94 (1954) 511–525.

[15] J.H. Ferziger, H.G. Kaper, Mathematical Theory of Transport Processes in Gases, North-Holland Publishing Company, Amsterdam, 1972.
[16] S.S. Lo, S.K. Loyalka, An efficient computation of near-continuum rarefied gas flows, Z. Angew. Math. Phys. (ZAMP) 33 (1982) 419–424.
[17] D. Valougeorgis, J.R. Thomas, Exact numerical results for Poiseuille and thermal creep flow in a cylindrical tube, Phys. Fluids 29 (2) (1986) 423–429.
[18] F. Sharipov, V. Seleznev, Rarefied gas flow through a long tube at any pressure ratio, J. Vac. Sci. Technol. A 12 (5) (1994) 2933–2935.